Supplemental Figures:

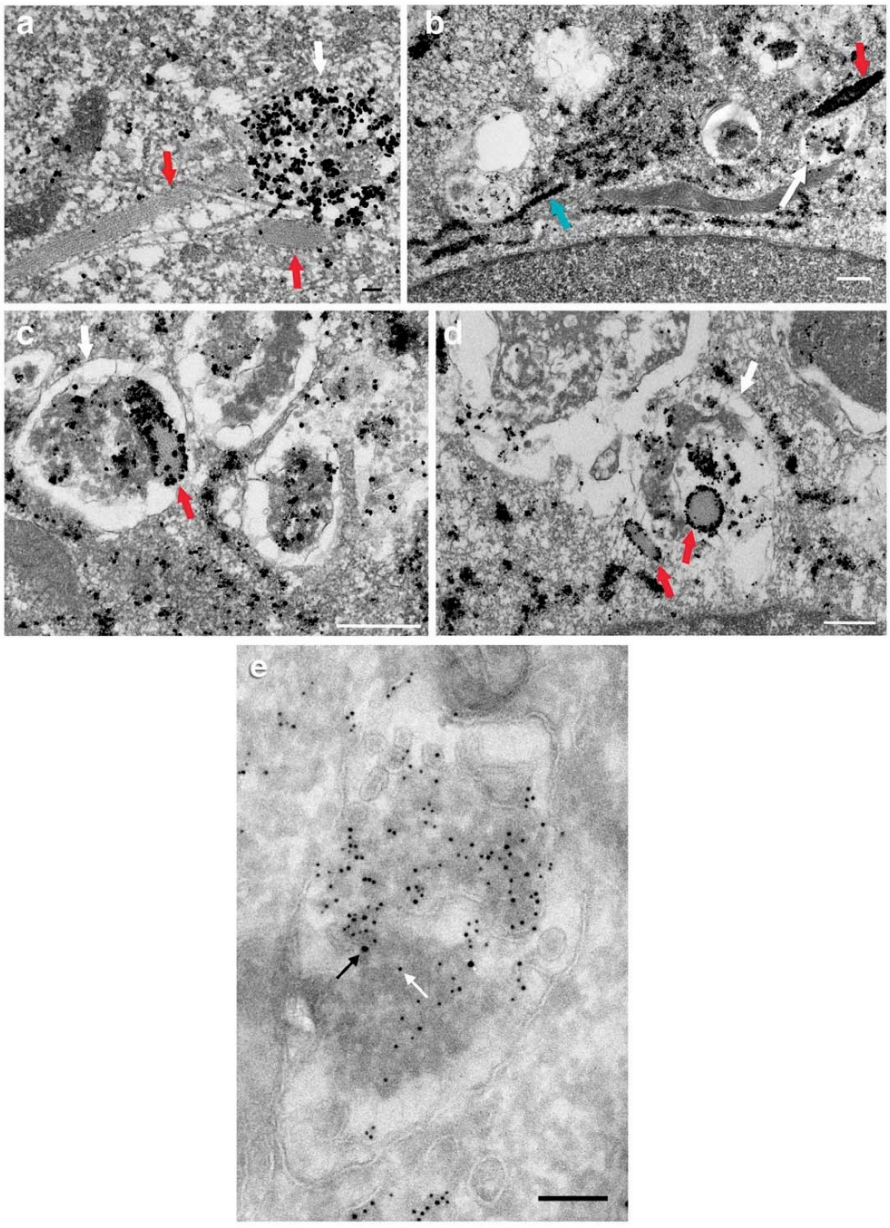

Figure 1: Intracellular distribution of VWF by electron microscopy in human endothelial cells.

a) Immunogold labeling of LC3 demonstrating an LC3-positive autophagosome (white arrow) very near and potentially fusing with two different WPBs (red arrows). **b**) Electron micrographs demonstrating immunogold labeling of the distribution of VWF within human endothelial cells. This subcellular distribution includes the endoplasmic reticulum (blue arrow), mature WPB (red arrow) and autophagosomes (white arrow). **c-d**) Immunogold labeling of VWF protein demonstrating WPBs (red arrows) and free VWF are contained within autophagosomes (white arrows). White scale bar equals 500 nm and black scale bar equals 100 nm. **e**) Dual cryo-immunogold labeling of an autophagosome. An electron micrographic image of an autophagosome found within a human endothelial cell. Dual immunogold labeling was employed using a secondary antibody conjugated with 10 nm gold particles (black arrow) directed against the LC3 primary antibody and a smaller (5 nm, white arrow) gold conjugated secondary antibody directed against the VWF primary antibody. Presence of large and small gold particles within the structure provides evidence for the presence of VWF within autophagosomes. Scale bar equals 100 nm.

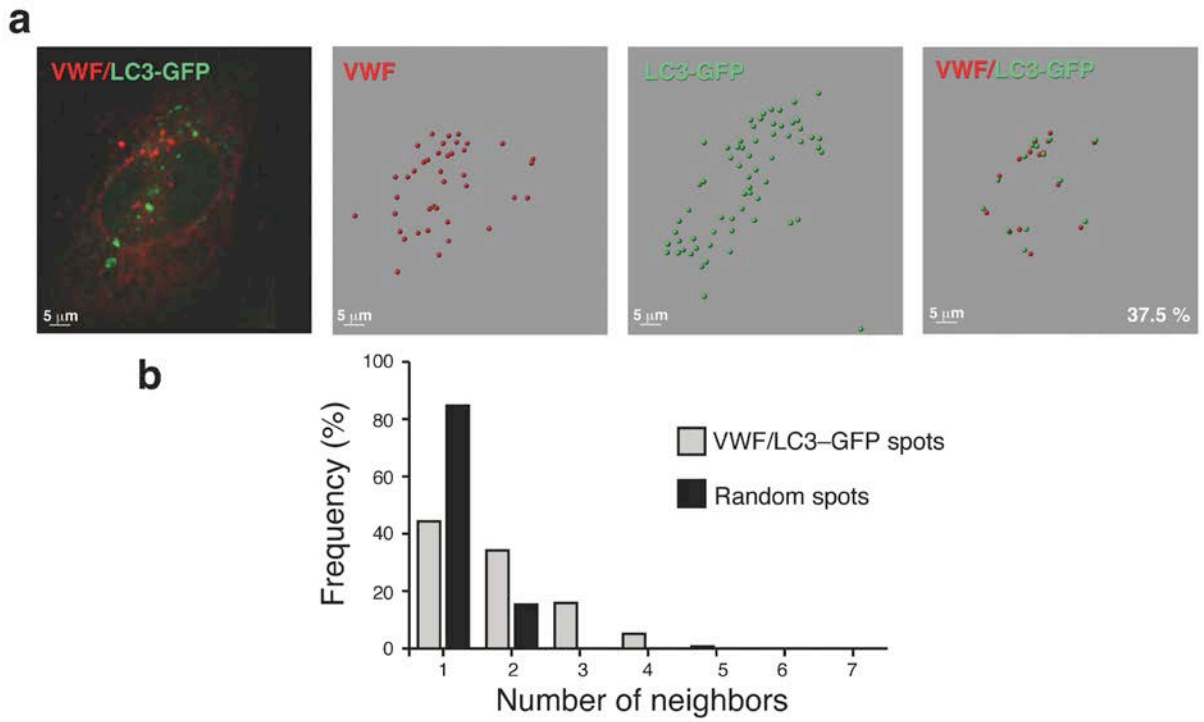

Figure 2: Clustering analysis of intracellular LC3 and VWF. **a**) Representative image analysis following immunofluorescent staining of human endothelial cells transfected with a LC3-GFP construct. Imaging software denotes the localization of spots greater than 1 μm in size and subsequent analysis allows for the determination of green (LC3) and red (VWF) spots with a centroid to centroid distance of less than 1.5 μm. In this example, this represents slightly over 37% of all spots. **b**) Statistical analysis of random nearest neighbor frequency. Clustering of LC3/VWF was analyzed by comparing experimental data (open bars) with a Monte Carlo simulation of randomly distributed spots of the same density in a similar volume (shaded bars). When examined by neighboring analysis, the observed LC3/VWF clustering distribution was greater than would be expected by chance (Mann-Whitney U test; $p < 0.01$, F test, $p < 0.01$).

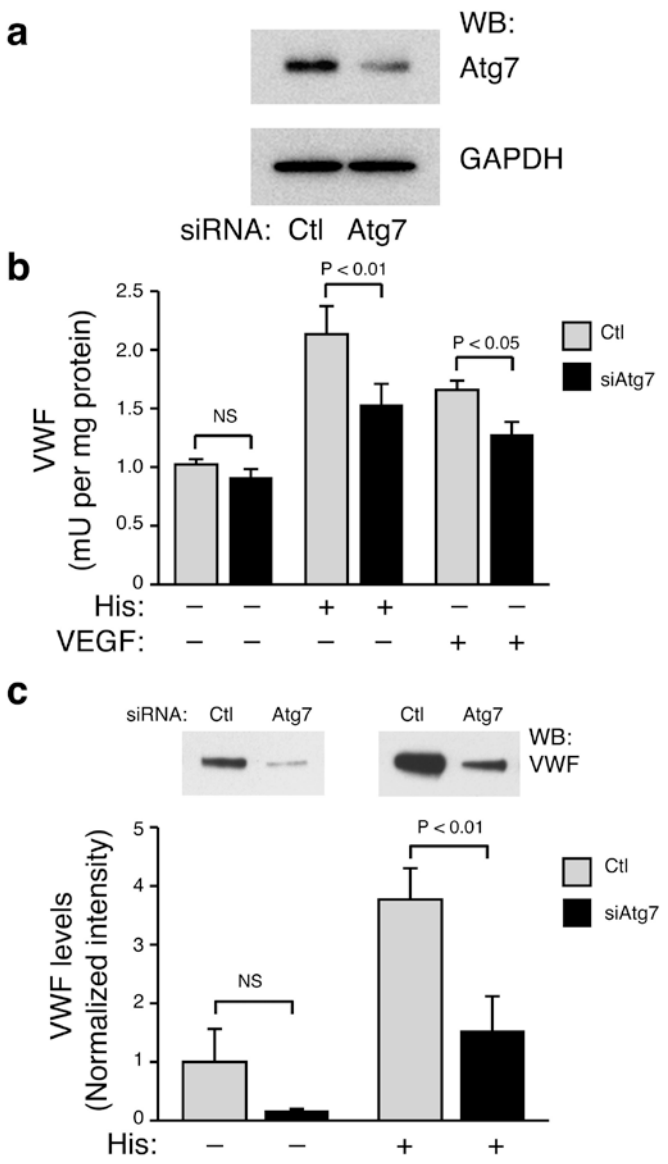

Figure 3: siRNA mediated knockdown of Atg7 inhibits VWF secretion. **a**) Atg7 expression following siRNA-mediated knockdown of Atg7. **b**) Secretion of VWF in control or Atg7 knockdown cells following stimulation with either histamine or VEGF (n=3 per condition). **c**) Western blot analysis of VWF secretion in control or Atg7 knockdown cells. Shown is one representative example (above) and quantitative summary of three independent Western blots (below).

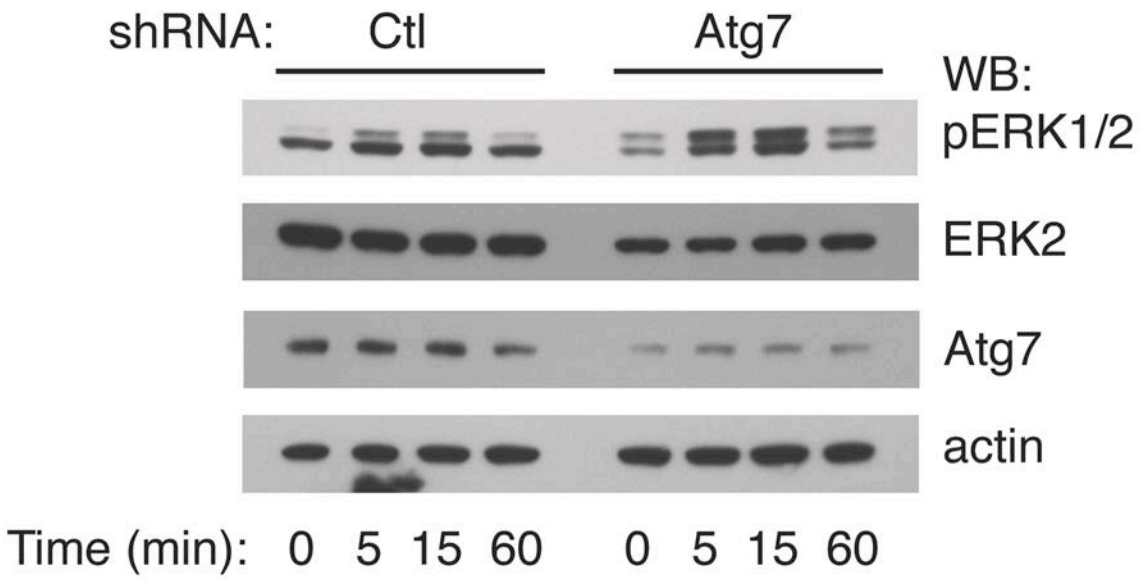

Figure 4: Inhibition of autophagy does not alter VEGF mediated signaling in endothelial cells. Control human endothelial cells or Atg7 shRNA knockdown human endothelial cells were stimulated with VEGF and phospho-ERK levels (pERK1/2) determined. VEGF-stimulated activation of ERK appears unaffected by Atg7 knockdown.

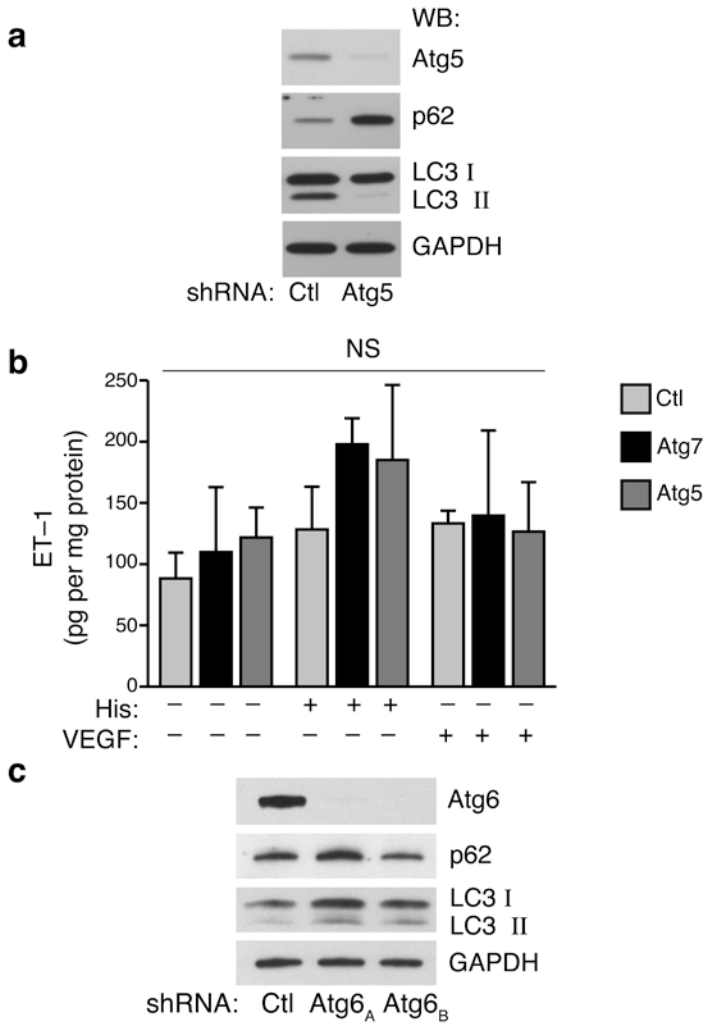

Figure 5: Western blot and functional analysis of Atg5, Atg6 and Atg7 knockdown. a) Western blot of human endothelial cells with control knockdown or following Atg5 shRNA mediated knockdown. Markers of the level of autophagic flux including p62 and LC3-II/LC3-I levels are shown. GAPDH is shown as a loading control. b) Endothelin-1 is known to be contained in part within WPBs. Stimulated release of Endothelin-1 was not altered by either Atg7 or Atg5 knockdown. Shown is one representative experiment performed in triplicate. c) Western blot analysis of Atg6 knockdown. Two independent shRNA for Atg6 are shown. Both shRNAs are effective in their knockdown of Atg6 however there appears to be only a very modest effect on overall macroautophagy.

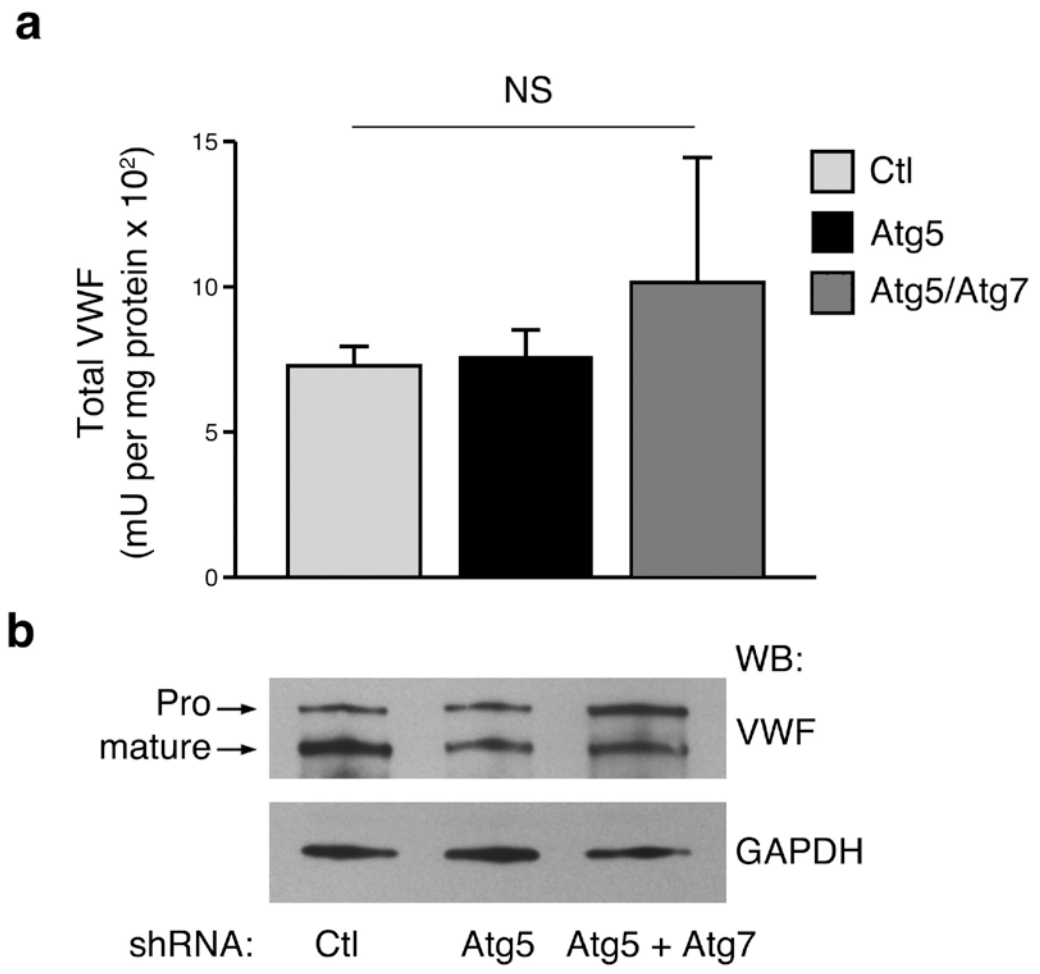

Figure 6: Effects of Atg7 and Atg5 on VWF. **a**) Intracellular VWF protein levels are not altered following knockdown of essential autophagy genes. Level of intracellular VWF protein was quantified by ELISA. Levels are shown for control knockdown cells, Atg5 knockdown alone or combined Atg5 and Atg7 knockdown. No significant difference was observed between these three groups, n=3 for each condition. **b**) Knockdown of Atg5 or combined knockdown of Atg5 and Atg7 results in an increase in the ratio of pro-VWF to mature VWF.

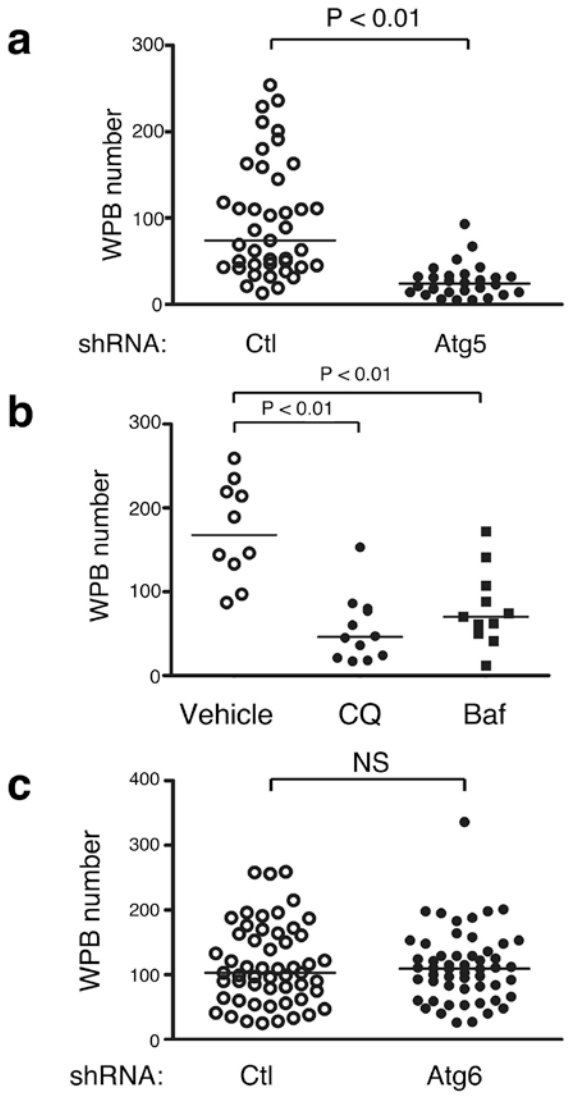

Figure 7: WPB number following either Atg5 or Atg6 knockdown or following treatment with pharmacological agents that inhibits autophagy. **a**) WPB number in control infected endothelial cells or following Atg5 knockdown. Analysis was performed by analyzing approximately 50 different cells for each condition. Lentiviral infection had an inhibitory effect on WPB number. **b**) WPB number in untreated human endothelial cells or in cells treated with chloroquine (CQ) or bafilomycin (Baf). **c**) Number of WPBs observed in control or Atg6 knockdown cells. No significant differences were observed ($n \geq 50$ per condition).

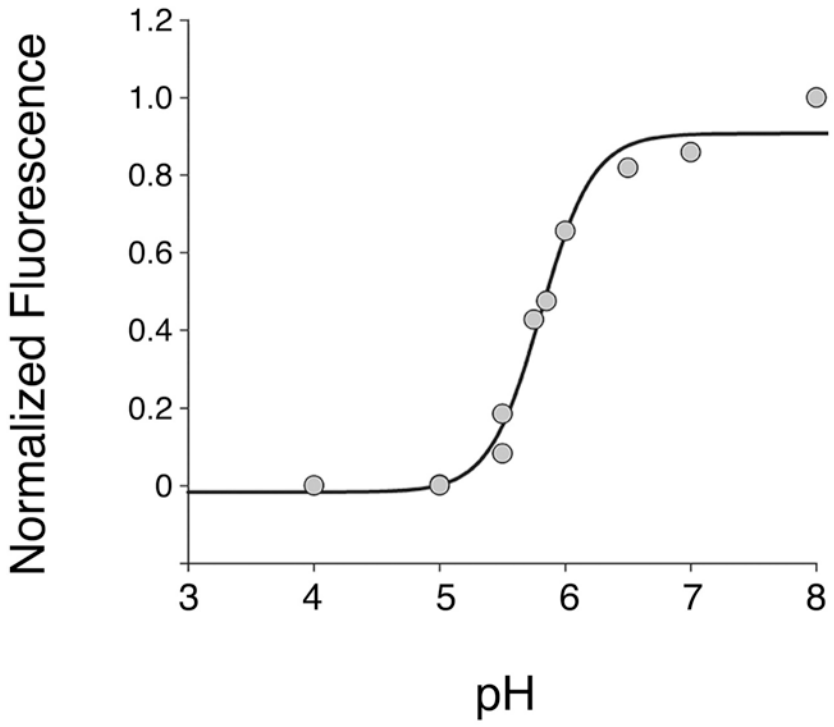

Figure 8: Calibration curve of VWF-mGFP fluorescence. Forty-eight hours after transfection, living HUVECs were analyzed over a large pH range and the fluorescence analyzed. Fluorescent intensity was normalized to the peak fluorescence obtained at pH 8.0.

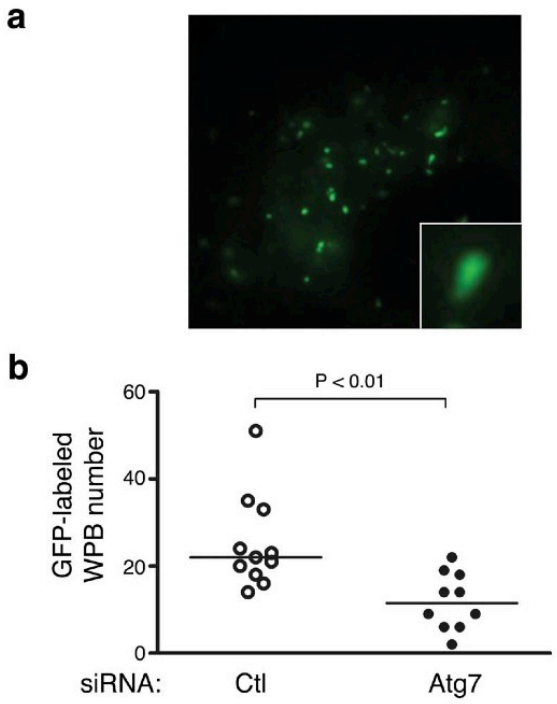

Figure 9: Analysis of secretion of WPBs containing VWF-GFP. **a**) Total internal reflection fluorescence (TIRF) image of human endothelial cell transfected with a construct encoding a VWF-GFP fusion protein. Inset is a high power view of a single VWF-GFP containing WPB. **b**) Cells expressing VWF-GFP were analyzed following a scrambled control or Atg7 specific knockdown. The number of fluorescently labeled WPBs was analyzed. As seen with other conditions, knockdown of Atg7 impaired the formation of mature WPBs.

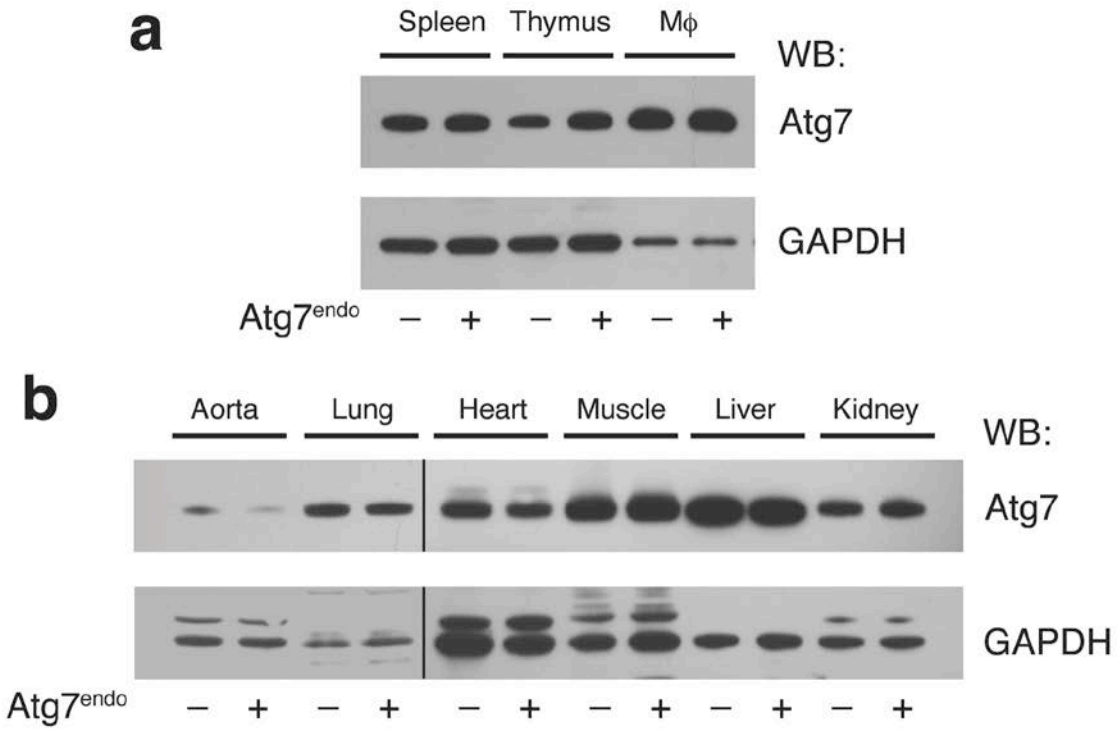

Figure 10: Atg7 expression in control or Atg7^{endo} mice. **a**) Atg7 levels in spleen, thymus or macrophages. **b**) Survey of Atg7 expression in various tissues. With the exception of the aorta, which presumably has a high percentage of endothelial cells per mg of total protein, overall Atg7 levels are not reduced in Atg7^{endo} mice. GAPDH or actin is used as a loading control.

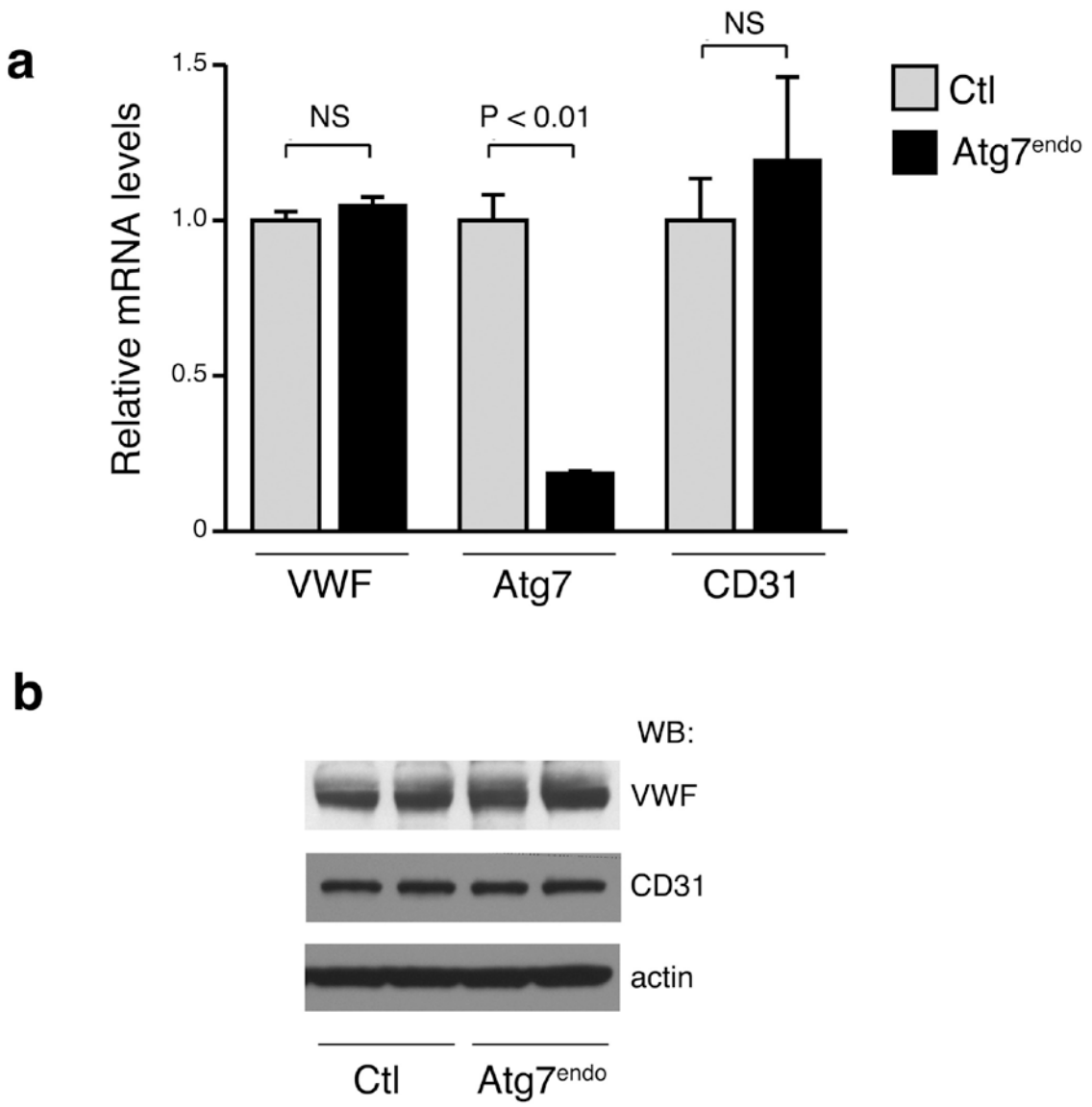

Figure 11: VWF expression in primary mouse endothelial cells and mice. **a**) Primary cultures of mouse endothelial cells were derived from either control or Atg7^{endo} mice. Relative levels of mRNA for VWF, Atg7 and CD31 (a marker of endothelial cell purity) were obtained. Deletion of Atg7 did not appear to alter VWF expression in mouse endothelial cells (n=3 replicates per genotype). **b**) Two aortic samples from either control mice or from Atg7^{endo} mice were analyzed for total VWF levels, expression of the endothelial protein CD31 and actin as a loading control.

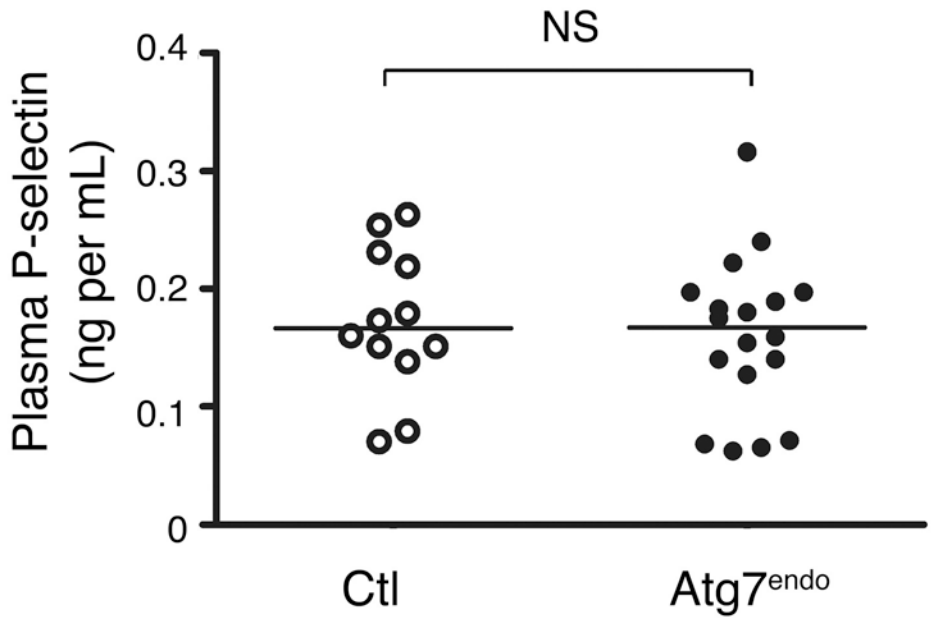

Figure 12: Analysis of plasma P-selectin levels. Circulating levels of P-selectin in either control mice or Atg7^{endo} mice. No significant differences were observed (n=12 for control and n=18 for Atg7^{endo} mice).

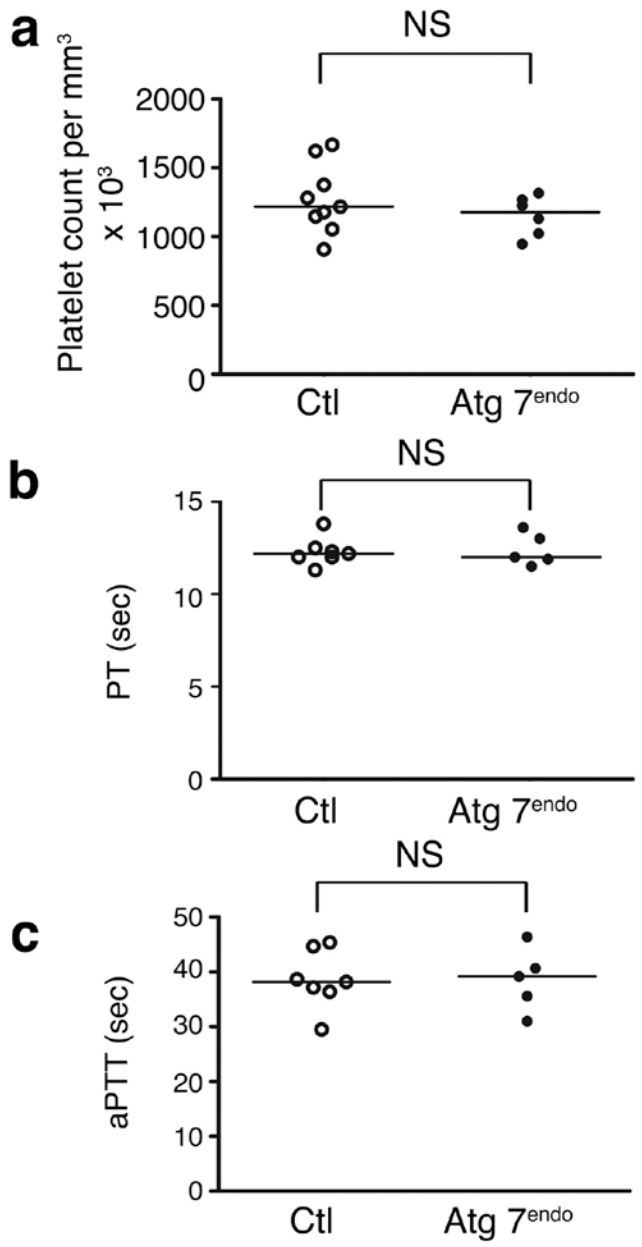

Figure 13: Analysis of hemostatic parameters in control and Atg7^{endo} mice. **a**) Although measured bleeding times were different, no significant differences in platelet number was observed between control (n=9) and Atg7^{endo} mice (n=6). **b**) Similarly, we observed no differences in measured Prothrombin time (PT: n=7 control mice and n=5 Atg7^{endo} mice) or **c**) Activated Partial Thromboplastin Time (aPTT: n=7 control mice and n=5 Atg7^{endo} mice).

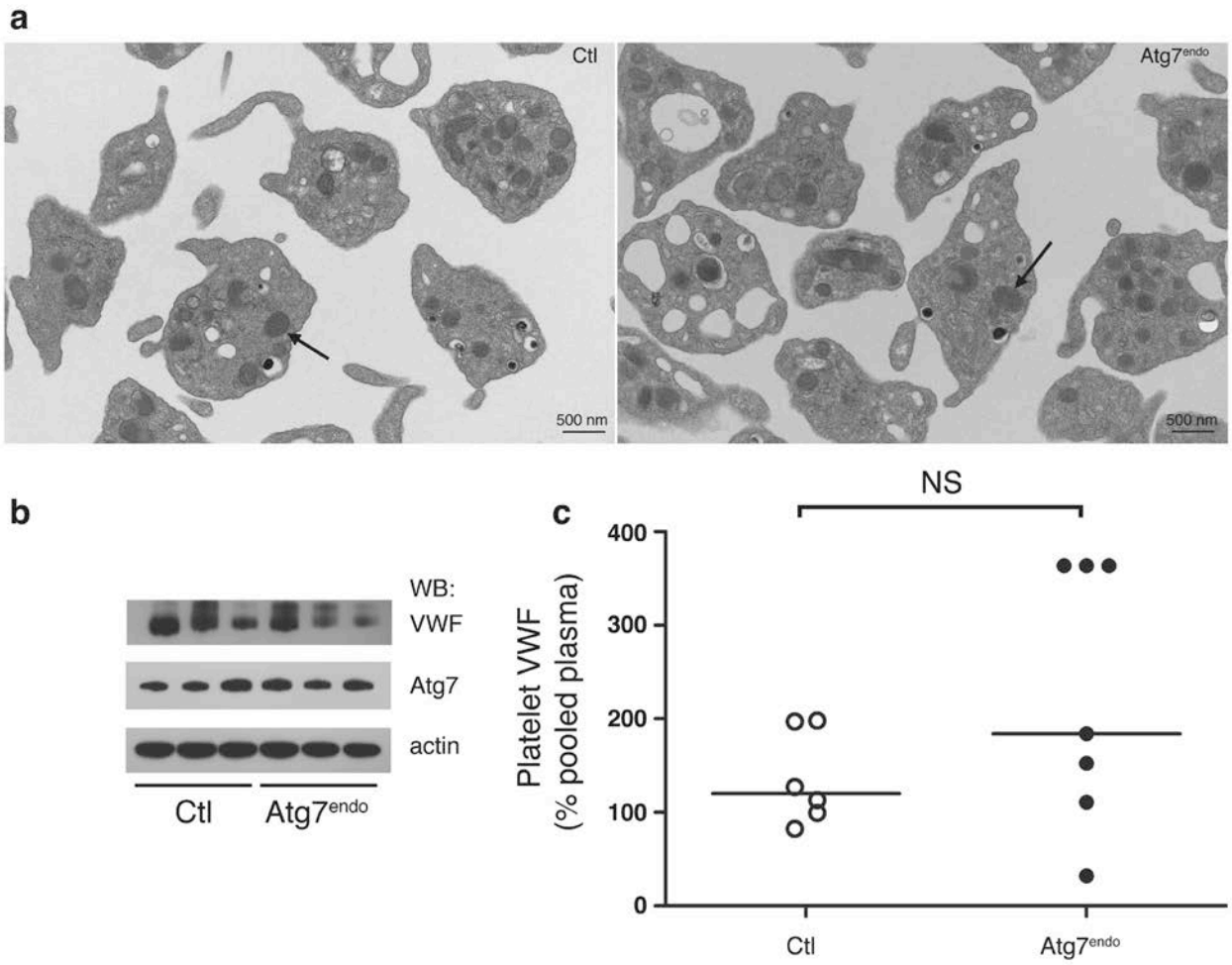

Figure 14: Deletion of Atg7 does not alter platelet VWF. **a**) Electron micrographs of control (left panel) and Atg7^{endo} platelets (right panel). Overall morphology was similar. Arrows indicate α-granules that contain VWF. **b**) Western blot levels of Atg7 and VWF in washed platelets obtained from three control or three Atg7^{endo} mice. **c**) VWF levels as determined by ELISA in platelets obtained from control (n=6) or Atg7^{endo} mice (n=7).

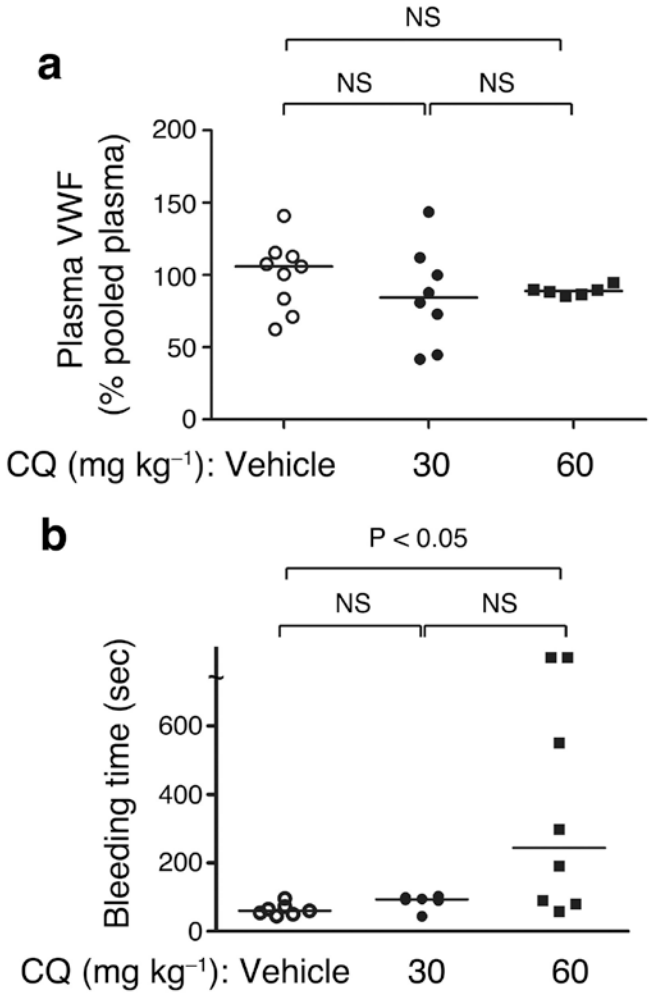

Figure 15: The effects of chloroquine treatment on VWF levels and measured bleeding times. **a**) Circulating VWF levels in vehicle treated (n= 9 mice) or mice given chloroquine (CQ) at either 30 mg/kg (n=8) or 60 mg/kg (n=6). Nine days after initiation of drug, levels of VWF in 129S1/SVIMJ mice were assessed. No significant differences were observed although there was a trend for reduced VWF in the CQ treated animals. **b**) Measured bleeding times for mice given the indicated dosage of chloroquine. The median bleeding times for mice treated with vehicle alone was 60 seconds, for 30 mg/kg of CQ it was 93.5 seconds and for 60 mg/kg of CQ it was 244.5 seconds. ($p<0.05$ between vehicle and CQ given at 60 mg/kg).